Available online at www.sciencedirect.com
ScienceDirect
Journal of the European Ceramic Society 27 (2007) 517–521
www.elsevier.com/locate/jeurceramsoc

Phase formation mechanism and characteristics of strontium barium niobate ceramics

Adelina Ianculescu [a,*], Ana Brăileanu [b], Georgeta Voicu [a], Ştefania Stoleriu [a]

[a] *Department of Oxide Materials Science and Engineering, University "Politehnica" Bucharest, 1-7 Gh. Polizu, P.O. Box 12-134, 011061 Bucharest, Romania*
[b] *Institute of Physical Chemistry "I.G. Murgulescu" of the Romanian Academy, 202 Spl. Independenţei, 060021 Bucharest, Romania*

Available online 5 June 2006

Abstract

Ceramic powders of $(1-x)BaNb_2O_6$–$xSrNb_2O_6$ $(0 \leq x \leq 1)$ composition were prepared by solid-state reaction. Thermal analysis data revealed that $SrNb_2O_6$ was formed at a lower temperature, compared with $BaNb_2O_6$. $Ba_{1-x}Sr_xNb_2O_6$ mixtures show an intermediate thermal behaviour. For the samples thermally treated at 1000 °C/3 h, X-ray diffraction data pointed out single phase compositions for $x = 0.4$–0.6, which means that $SrNb_2O_6$ completely dissolves into $BaNb_2O_6$ lattice in this composition range The temperature increase at 1150 °C leads to partial decomposition and supplementary demixing phenomena for all the mixtures analyzed. At 1300 °C, solid-state reactions progress and a structural rearrangement occurs, so that the same phase composition identified at 1000 °C was found again. A slight increase of the isomorphy limit of $SrNb_2O_6$ into $BaNb_2O_6$ lattice was also noticed. Single-phase compositions were identified for the samples with $x = 0.3$–0.6.

Keywords: Powders-solid state reaction; Sintering; X-ray methods; Niobates; Phase formation

1. Introduction

Among ferroelectric relaxor materials, strontium barium niobate solid solutions $Ba_{1-x}Sr_xNb_2O_6$ (BSN) having a tungsten bronze type structure are of importance in many applications such as electro-optic, pyroelectric, piezoelectric and photorefractive devices.[1–7] Despite the technological applications of these materials, only a few works deal with the formation mechanism of $Ba_{1-x}Sr_xNb_2O_6$ solid solutions, which remains still controversial.[8,9]

This work represents an attempt to clarify some aspects of phase formation of mixed crystals in $BaNb_2O_6$–$SrNb_2O_6$ system.

2. Experimental

2.1. Samples preparation

The raw materials were p.a. grade oxides and carbonates: Nb_2O_5 (Johnson Matthey Clemicals Ltd.), $SrCO_3$ (Fluka) and $BaCO_3$ (Fluka). Mixtures of $(1-x)BaNb_2O_6$–$xSrNb_2O_6$ $(0 \leq x \leq 1)$ composition, presented in Fig. 1, were prepared by classical ceramic method, by a wet homogenization technique in isopropyl alcohol.

The initial mixtures were used as powdered samples for non-isothermal investigations. For isothermal investigations, pellets, 20 mm diameter and ~3 mm thickness were prepared by uniaxially pressing at 160 MPa. The pellets were sintered for 3 h at 1000, 1150 and 1300 °C.

2.2. Samples characterization

Thermal analyses (TG and DTG) were used in order to establish the formation mechanism of the compounds and/or solid solutions studied, using a Shimadzu analyzer DTG-TA-51H, up to 1000 °C.

Phase composition evolution in isothermal conditions was investigated by X-ray diffraction by means of a Shimadzu XRD 600 diffractometer.

3. Results and discussion

3.1. Non-isothermal treatments

For the mixture corresponding to $BaNb_2O_6$ composition, the processes noticed with the temperature raise occur with weight

* Corresponding author. Tel.: +40 21 4023848; fax: +40 21 3181010.
E-mail address: a.ianculescu@rdslink.ro (A. Ianculescu).

0955-2219/$ – see front matter © 2006 Elsevier Ltd. All rights reserved.
doi:10.1016/j.jeurceramsoc.2006.04.109

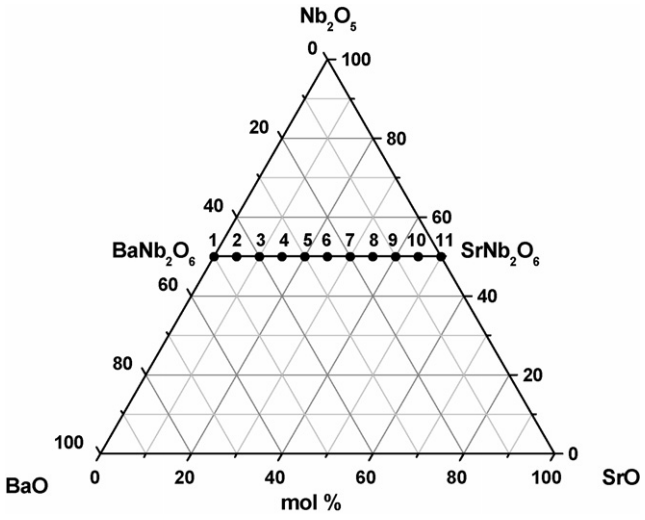

Fig. 1. Position of the compositions investigated in the ternary system $BaO–SrO–Nb_2O_5$.

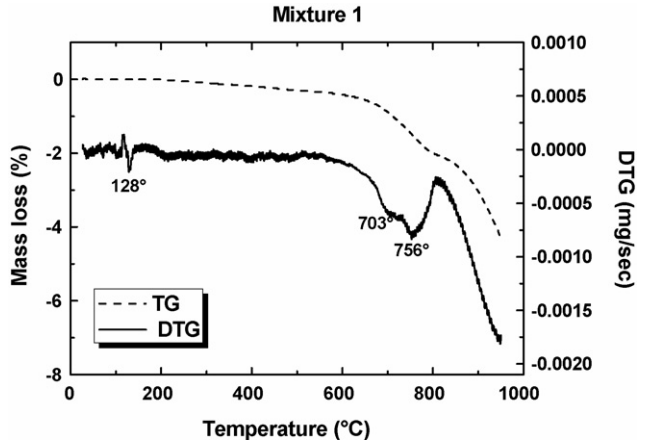

Fig. 2. TG/DTG curves of $BaNb_2O_6$.

losses in several distinct steps (Fig. 2). In the temperature range of 600–800 °C, DTG curve shows the presence of three distinct decomposition steps, corresponding probably to $BaCO_3$ decomposition simultaneously with $BaNb_2O_6$ formation.

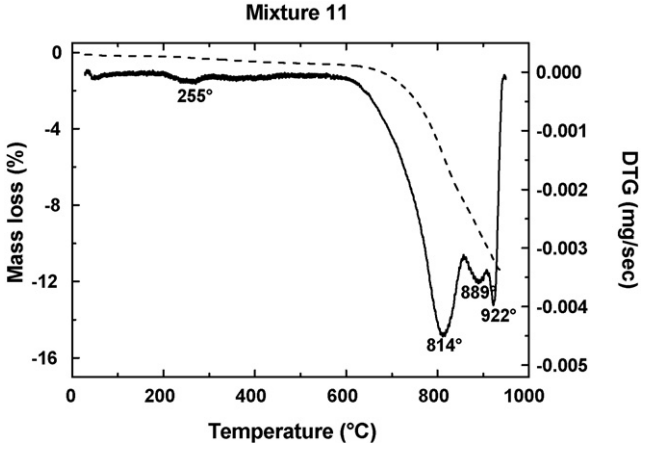

Fig. 3. TG/DTG curves of $SrNb_2O_6$.

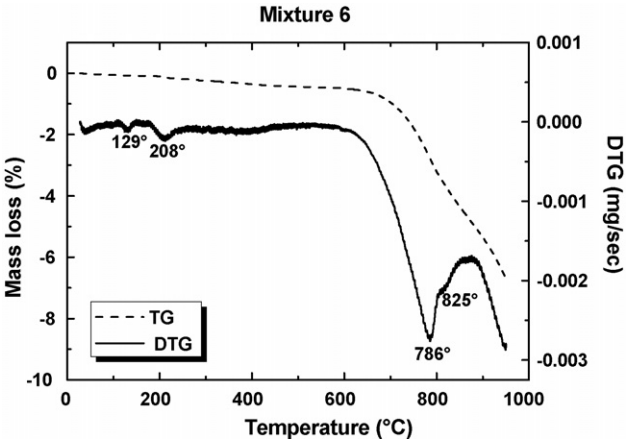

Fig. 4. TG/DTG curves of $Ba_{0.5}Sr_{0.5}Nb_2O_6$.

Similarly, DTG curve for $SrNb_2O_6$ composition (Fig. 3) emphasizes three decomposition steps with the main one between 650 and 850 °C, unlike to the former composition which exhibits the main weight loss between 830 and 980 °C. This suggests that $SrNb_2O_6$ develops at lower temperatures compared to $BaNb_2O_6$, which explains the presence of secondary phases identified in the mixture corresponding to $BaNb_2O_6$ formula at 1000 °C.

For the equimolar composition (Fig. 4) one can observe also the weight losses due to the carbonates decomposition in several steps, but less distinct comparatively with $BaNb_2O_6$ composition.

3.2. Isothermal treatments

3.2.1. $BaNb_2O_6$ composition

Phase composition at 1000 °C (Fig. 5) shows the presence, beside of a major $BaNb_2O_6$ phase (JCPDS 77-05890), of some non-equilibrium Nb-rich $Ba_3Nb_{10}O_{28}$ (JCPDS 13-0575), Ba-rich $Ba_5Nb_4O_{15}$ (JCPDS 17-0794) compounds, Nb_2O_5 (JCPDS

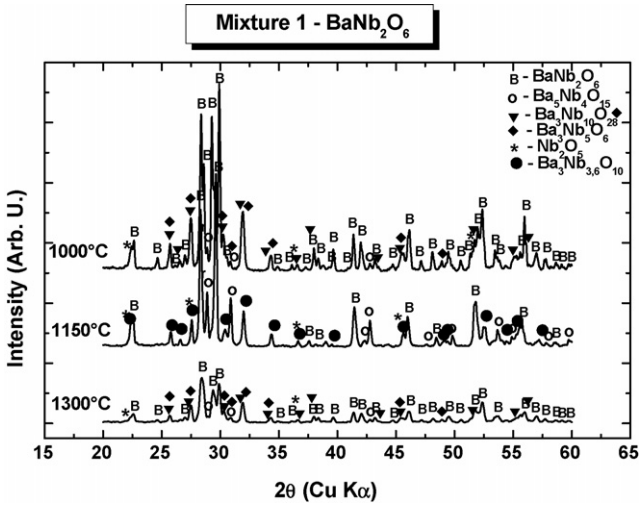

Fig. 5. X-ray diffraction patterns of the composition $BaNb_2O_6$ isothermally treated at 1000, 1150 and 1300 °C.

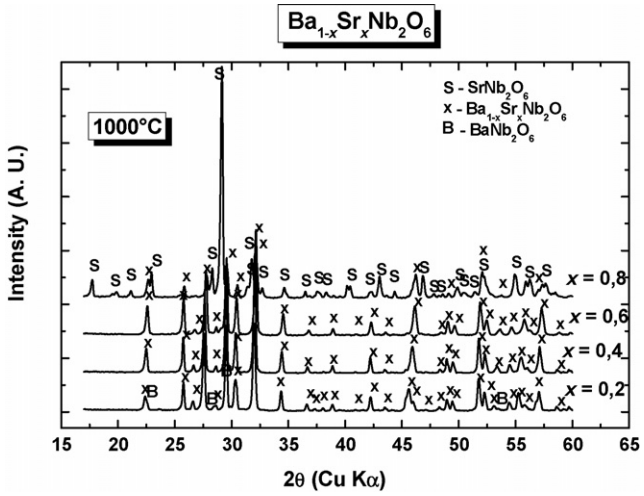

Fig. 6. X-ray diffraction patterns of the compositions with $x = 0.2$–0.8, isothermally treated at 1000 °C.

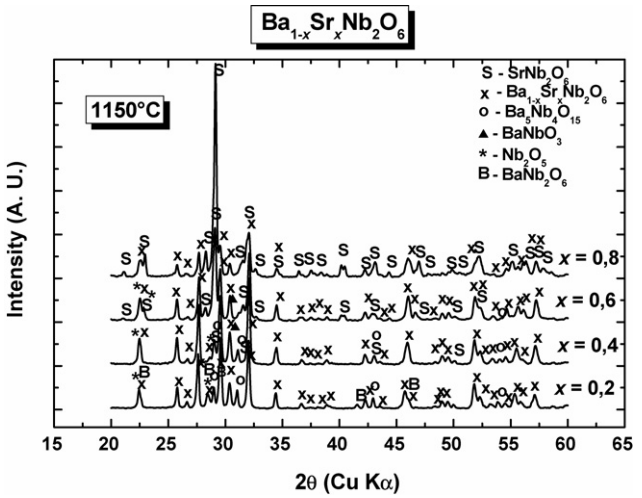

Fig. 7. X-ray diffraction patterns of the compositions with $x = 0.2$–0.8, isothermally treated at 1150 °C.

37-1468), as well as of some compounds close to $BaNb_2O_6$ stoichiometry such as $Ba_3Nb_5O_6$ (JCPDS 31-0158).

Surprisingly, at 1150 °C, X-ray diffraction data indicates that in the 1000–1150 °C temperature range $BaNb_2O_6$ decomposition occurs, pointed out by the significant decreasing of all characteristic diffraction maxima of this compound. At the same time, the vanishing of $Ba_3Nb_{10}O_{28}$ and $Ba_3Nb_5O_6$ and the formation of $BaNb_{3.6}O_{10}$ (JCPDS 46-0942) was observed. More intense maxima corresponding to $Ba_5Nb_4O_{15}$ and Nb_2O_5 phases were recorded, suggesting the instability of $Ba_3Nb_{10}O_{28}$ and the possible consumption of $BaNb_2O_6$ either for $BaNb_{3.6}O_{10}$ formation or for $Ba_5Nb_4O_{15}$ development, or both.

The temperature raise at 1300 °C indicates the diminution of major $BaNb_2O_6$ phase but the quantitative increase of $Ba_5Nb_4O_{15}$. $BaNb_{3.6}O_{10}$, identified at 1150 °C and stable in a very narrow temperature range, was not identified at 1300 °C, probably due to a solid-state incongruence with Nb_2O_5 and $Ba_3Nb_{10}O_{28}$ reforming. The important decrease of the diffraction maxima of the major $BaNb_2O_6$ phase shows that a higher temperature does not enhance its crystallization but, on the contrary, affects the lattice crystallinity.

3.2.2. $Ba_{0.8}Sr_{0.2}Nb_2O_6$ composition

At 1000 °C, a solid solution structurally very close to $Ba_{0.67}Sr_{0.33}Nb_2O_6$ (JCPDS 73-0126) was identified (Fig. 6). In this solid solution the atomic ratio Ba/Sr = 2, compared to Ba/Sr = 4 in the initial mixture so that the supplementary Ba segregates as a secondary phase solid solution with $BaNb_2O_6$ structure (BNss).

The ternary solid solution BSNss changes its composition (from $Ba_{0.67}Sr_{0.33}Nb_2O_6$ to $Ba_{0.5}Sr_{0.5}Nb_2O_6$) in the 1000–1150 °C temperature range (Fig. 7) and becomes poorer in Ba (Ba/Sr varies from 2 to 1), suggesting an obvious demixing tendency with supplementary $BaNb_2O_6$ solid solution (BNss) formation. Also, a decomposition trend of a small $BaNb_2O_6$ quantity, with the formation of some secondary phases such as $Ba_5Nb_4O_{15}$ and Nb_2O_5 was noticed.

In the 1150–1300 °C temperature range, a structural rearrangement, by the incorporation of BNss into BSNss lattice occurs, the mixed crystals becoming Ba-richer (Fig. 8). The characteristic diffraction maximum of BNss is still present due to its formation by the consumption of the intermediate phases $Ba_5Nb_4O_{15}$ and Nb_2O_5. A diminution of the characteristic diffraction peaks of BSNss with the temperature rise was observed, too, because of the ternary solid solution decomposition followed by its reforming.

3.2.3. $Ba_{0.5}Sr_{0.5}Nb_2O_6$ composition

At 1000 °C, a single crystalline phase, $Ba_{0.5}Sr_{0.5}Nb_2O_6$ was detected (Fig. 9), obtained either by the independent formation of $BaNb_2O_6$ and $SrNb_2O_6$, which react subsequently with $Ba_{0.5}Sr_{0.5}Nb_2O_6$ formation or by the simultaneous decomposition of $BaCO_3$ and $SrCO_3$ with the single step formation of $Ba_{0.5}Sr_{0.5}Nb_2O_6$.

A decrease of the crystallinity degree and of the quantity of the main phase was noticed at 1150 and 1300 °C. At

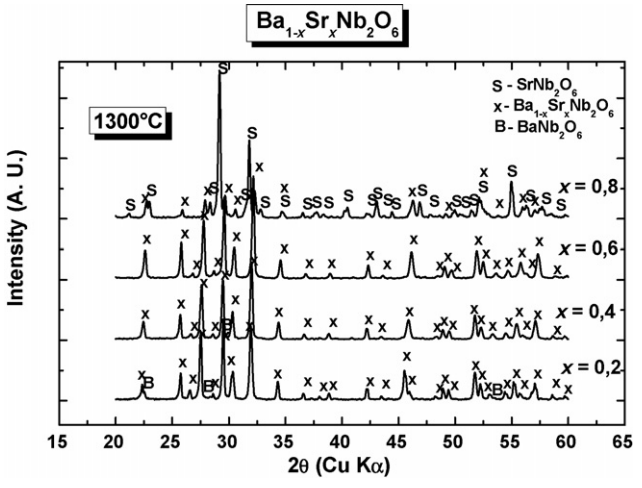

Fig. 8. X-ray diffraction patterns of the compositions with $x = 0.2$–0.8, isothermally treated at 1300 °C.

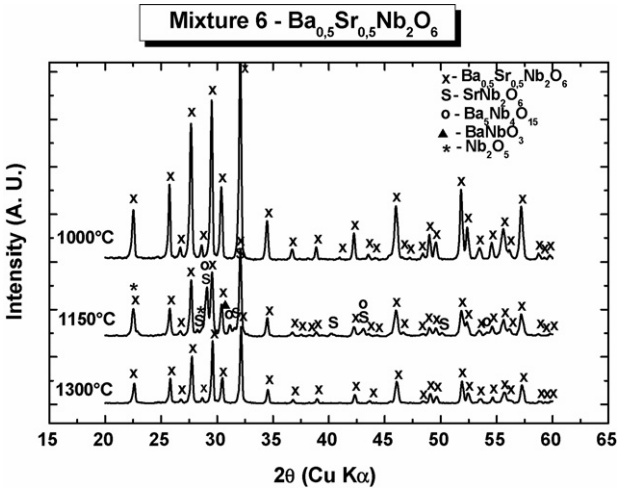

Fig. 9. X-ray diffraction patterns of the composition $Ba_{0.5}Sr_{0.5}Nb_2O_6$, isothermally treated at 1000, 1150 and 1300 °C.

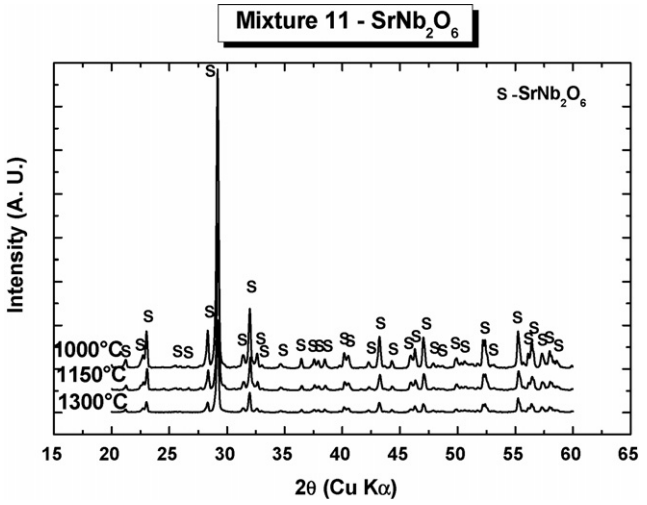

Fig. 10. X-ray diffraction patterns of the composition $SrNb_2O_6$, isothermally treated at 1000, 1150 and 1300 °C.

1150 °C, a supplementary phase with the structure of $SrNb_2O_6$ solid solution (SNss), as well as some intermediate phases ($Ba_5Nb_4O_3$, $BaNbO_3$ and Nb_2O_5) were identified, suggesting that $Ba_{0.5}Sr_{0.5}Nb_2O_6$ solid solution demixes with $SrNb_2O_6$ segregation. $BaNb_2O_6$ excess, present in the ternary solid solution, decomposes, leading to the above-mentioned residual phases.

The single phase $Ba_{0.5}Sr_{0.5}Nb_2O_6$ was again identified at 1300 °C.

3.2.4. $Ba_{0.2}Sr_{0.8}Nb_2O_6$ composition

The solid solution formed at 1000 °C is structurally close to the composition indexed as $Ba_{0.5}Sr_{0.5}Nb_2O_6$, with Ba/Sr = 1 (Fig. 6). Taking into account that the initial Ba/Sr = 1/4, one finds out that Sr is prevalent bounded (approximately 3/4) in $SrNb_2O_6$, otherwise identified as major phase and only 1/4 of the total Sr is bounded in the ternary BSNss. The mixed crystals can result either indirectly by the reaction of $BaNb_2O_6$ and $SrNb_2O_6$ (obtained by the decomposition of the both carbonates) or directly by the reaction of the raw materials. Considering the fact that $BaNb_2O_6$ and $SrNb_2O_6$ have different structures ($BaNb_2O_6$ is orthorhombic and $SrNb_2O_6$ is tetragonal), due to the significant difference between the ionic radii of Ba^{2+} and Sr^{2+}, it is much more probable the independent formation of the both limit components and their further mutual incorporation than the direct single step formation of BSNss. Our results are in agreement with those of Fang et al.[8] but differ by the data reported by Hirano et al.[9]

The increase of the temperature at 1150 °C enhances the demixing tendency of BSNss, revealed by an increased ratio of the SNss/BSNss diffraction intensities due to the distortions caused by the important diffusion of Sr (Fig. 7).

In the 1150–1300 °C temperature range, it comes out that a rearrangement in a tungsten bronze structure, with the diminution of the SNss/BSNss ratio, comparatively with 1000 °C, occurs (Fig. 8). This suggests an increase of the isomorphy limit at 1300 °C. At the same time, one can notice an overall diminution of the diffraction intensities for the both solid solutions, at 1300 °C, due to a lower crystallinity resulted as a consequence of the structural disordering.

3.2.5. $SrNb_2O_6$ composition

Starting with 1000 °C, a single phase, $SrNb_2O_6$, with tungsten bronze structure, is obtained (Fig. 10). The temperature raise at 1150 and then at 1300 °C does not change the phase composition. However, one can remark a diminution of the crystallinity degree of the compound with the increase of the temperature, but much less obvious comparatively with $BaNb_2O_6$.

Concerning the evolution of the phase composition of all the ceramics studied, related to Sr substitution, at various temperatures, some aspects have to be emphasized.

At 1000 °C, a $Ba_{1-x}Sr_xNb_2O_6$ phase with a various chemical composition as a function of the substitution degree was detected. Thus, for $x = 0.2$, the solid solution is compositionally closer to the formula $Ba_{0.67}Sr_{0.33}Nb_2O_6$, whereas for $x = 0.5$ and 0.8, BSNss corresponds rather to $Ba_{0.5}Sr_{0.5}Nb_2O_6$ composition. At the same time, for $x = 0.8$, the isomorphy limit is reached, since a demixing of this solid solution occurs with SNss segregation.

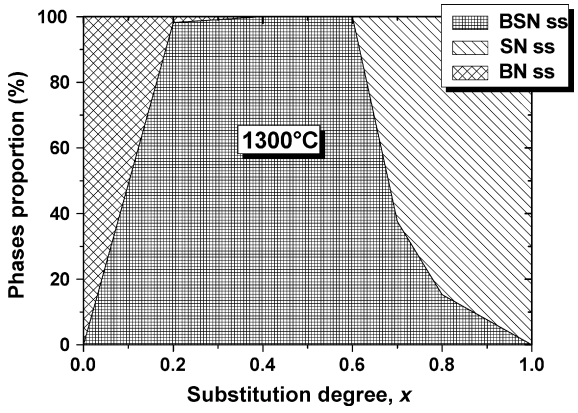

Fig. 11. The quantitative evolution of the three solid solutions, BNss, SNss and BSNss, vs. Sr content, at 1300 °C.

No single-phase composition was noticed at 1150 °C for all samples studied, except $SrNb_2O_6$. Thus, for $x = 0.8$, the same demixing process, pointed out at 1000 °C was remarked. For $x = 0.5$, a secondary phase, SNss, as well as secondary phases $Ba_5Nb_4O_3$, $BaNbO_3$ and Nb_2O_5 were identified. For $x = 0.2$, beside intermediate phases such as $Ba_5Nb_4O_3$ and Nb_2O_5, BNss was also detected.

At 1300 °C, only for $x = 0.5$ a single phase $Ba_{0.5}Sr_{0.5}Nb_2O_6$ was identified. For $x = 0.2$, the reforming of both $BaNb_2O_6$ and $Ba_{0.67}Sr_{0.33}Nb_2O_6$ was pointed out, while for $x = 0.8$, beside $SrNb_2O_6$ major phase a BSNss significantly lower from quantitative point of view, was detected.

Fig. 11 presents the quantitative evolution of the three solid solutions: BNss, SNss and BSNss, as a function of Sr substitution degree at 1300 °C.

4. Conclusions

Thermal analysis data reveal that $SrNb_2O_6$ forms at lower temperature than $BaNb_2O_6$. Mixtures corresponding to $Ba_{1-x}Sr_xNb_2O_6$ show an intermediate thermal behaviour.

Unlike the mixture corresponding to $SrNb_2O_6$ formula, which is single phase starting with 1000 °C, the mixture corresponding to $BaNb_2O_6$ formula shows at the same temperature a more complex phase composition consisting, beside $BaNb_2O_6$, of several non-equilibrium compounds resulted from the reaction between $BaCO_3$ and Nb_2O_5. For the other mixtures thermally treated at 1000 °C, partial isomorphy, with demixing regions, both in the Ba-rich zone (for $x = 0$–0.4, with BNss formation) and Sr-rich zone (for $x = 0.6$–1, with SNss formation) of the $BaNb_2O_6$–$SrNb_2O_6$ system was observed. Single-phase compositions were detected only for mixtures with x ranged between 0.4 and 0.6.

At 1150 °C, decomposition and demixing phenomena take place for all the samples analyzed, excepting $SrNb_2O_6$ composition; no-single phase solid solutions were identified. This instability is more obvious for Ba-rich mixtures, in which even BNss partially decomposes in several non-equilibrium compounds. For the compositions closer to the equimolar $BaNb_2O_6/SrNb_2O_6$ ratio ($x = 0.4$–0.6) a Sr-rich solid solution (SNss) segregates.

At 1300 °C, solid-state reactions progress and a structural rearrangement occurs, so that the same phase composition identified at 1000 °C was found again. A slight increase of the single-phase region toward the Ba-rich side of the $BaNb_2O_6$–$SrNb_2O_6$ system was noticed. However, in comparison with 1000 °C, at 1300 °C all the samples exhibit lower crystallinity.

References

1. Lenzo, P. V., Spencer, E. G. and Ballman, A. A., Electro-optic coefficients of ferroelectric strontium barium niobate. *Appl. Phys. Lett.*, 1967, **11**, 23–24.
2. Glass, A. M., Investigation of the electrical properties of $Sr_{1-x}Ba_xNb_2O_6$ with special reference to pyroelectric detection. *J. Appl. Phys.*, 1969, **40**, 4699–4713.
3. Neurgaonkar, R. R., Kalisher, M. H., Lim, T. C., Staples, E. J. and Keester, K. L., Czochralski single-crystal growth of $Sr_{.61}Ba_{.39}Nb_2O_6$ for surface acoustic wave applications. *Mater. Res. Bull.*, 1980, **15**, 1235–1240.
4. Thaxter, J. B., Electrical control of holographic storage in strontium barium niobate. *Appl. Phys. Lett.*, 1969, **15**, 210–212.
5. Neurgaonkar, R. R. and Cory, W. K., Progress in photorefractive tungsten bronze crystals. *J. Opt. Soc. Am. B: Opt. Phys.*, 1986, **3**, 274–282.
6. Duran, C., Trolier-McKinstry, S. and Messing, G. L., Fabrication and electrical properties of texture $Sr_{0.53}Ba_{0.47}Nb_2O_6$ ceramics by templated grain growth. *J. Am. Ceram. Soc.*, 2000, **83**, 2203–2213.
7. Li, M.-H., Chong, T.-C., Xu, X.-W. and Kumagai, H. J., Structural and dielectric investigation of doped $Sr_{0.61}Ba_{0.39}Nb_2O_6$ crystals. *J. Appl. Phys.*, 2001, **89**, 5644–5646.
8. Fang, T.-T., Wu, N.-T. and Shiau, F.-S., Formation mechanism of strontium barium niobate ceramic powders. *J. Mater. Sci. Lett.*, 1994, **13**, 1746–1748.
9. Hirano, S.-I., Yogo, T., Kikuta, K.-I. and Ogiso, K.-J., Preparation of strontium barium niobate by sol–gel method. *J. Am. Ceram. Soc.*, 1992, **75**, 1697–1700.